

# Field measurements of pressure characteristics for components in a hybrid ventilation system

<sup>1</sup>Wachenfeldt B. J., <sup>2</sup>Tjelflaat P. O. <sup>2</sup>Shahriari B.Z.

<sup>1</sup>*Sintef Civil and Environmental Engineering, Architecture and Building Technology, 7465 Trondheim, Norway.*

<sup>2</sup>*Norwegian University for Science and Technology, Dept.of Energy and process engineering, Kolbjoern Hejes vei 1b, 7491 Trondheim, Norway*

## Contents

Abstract .....	1
1 Introduction .....	2
2 The field experiment.....	2
2.1 Pressure differentials.....	3
2.2 Airflow rates .....	4
3 Results and characterisation of the ventilation system components.....	5
3.1 Pressure drop across the intake unit.....	6
3.2 Pressure drop across the filter .....	7
3.3 Pressure drop across the combined heat recovery and heating coil .....	8
3.4 Pressure drop from the distribution duct to the extract chamber .....	9
3.5 Pressure drop out through the roof tower.....	9
3.6 Fan characteristics.....	11
3.7 System pressure characteristics.....	13
4 Conclusions .....	15
5 References .....	15

## Abstract

A detailed field experiment has been carried out in order to investigate the hybrid ventilation system in the Mediå School in Grong, Norway. The total airflow rate and the pressure differentials over the various components and airflow openings have been accurately measured. Mathematical formulae describing their pressure characteristics have been derived from the results enabling easy implementation into computer simulation tools with inter-zone airflow network models. The total pressure drop for the whole ventilation system was derived as  $\Delta P = 29.1Q + 2.3Q^2$  [Pa], where  $Q$  [m<sup>3</sup>/s] is the airflow rate. This indicates that laminar rather than turbulent flow dominates. The results also show that it is fully possible to use regular mechanical ventilation components such as filters and heat exchangers in a system based purely on natural driving forces.

# 1 Introduction

Natural and hybrid ventilation has during the last decade experienced a renaissance in Europe. The penalty of electrical energy use in traditional mechanical ventilation and air conditioning is the main reason. Successful design of such ventilation systems requires knowledge about the pressure characteristics of components.

Components made for conventional ventilation systems can be applied in natural and hybrid ventilation systems. However, those components are until now not supplied with data for the low air velocities in natural and hybrid ventilation.

A field experiment was carried out in order to obtain accurate measurements of pressure differentials over all the components in the ventilation airflow path of the *Mediå School* in Grong, Norway (64.5 N; 12.5 E). The building has demand controlled displacement ventilation provided through utilisation of thermal buoyancy supported by an axial supply and extract fan. CO<sub>2</sub>-sensors placed in all the classrooms give input to the control algorithm controlling exhaust dampers placed in all the rooms and activating the fans when necessary. The building is a case study in the International Energy Agency - Energy Conservation in Buildings and Community Systems (IEA ECBCS) Annex 35: "Hybrid Ventilation in New and Retrofitted Office Buildings"[1].

## 2 The field experiment

The main experiment was carried out during a 14-hour period from 16:00 on October 31 till 06:00 on November 1, 2002. The weather forecast was considered before selecting this period. Conditions during the experiment were ideal, with very low winds, only minor changes in outdoor temperature and no occupancy in the school.

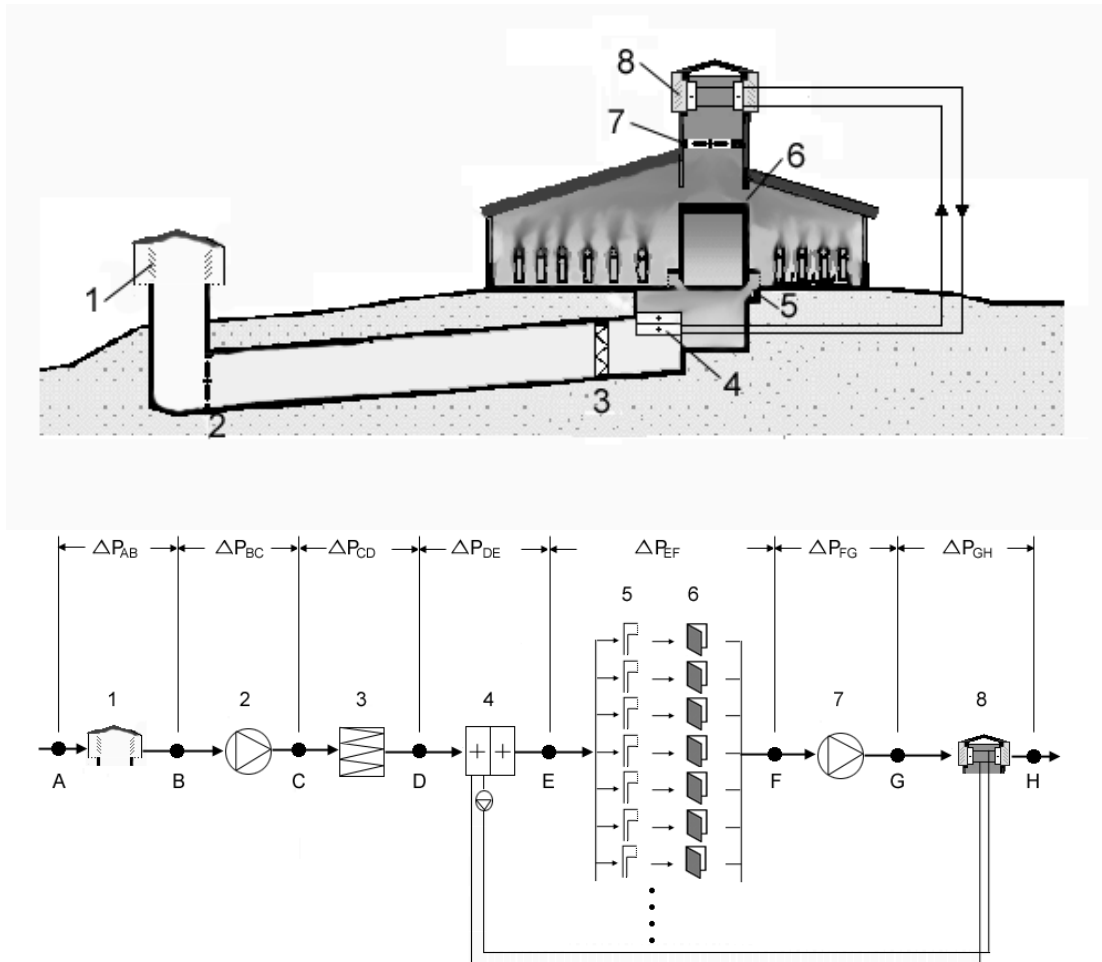


Figure 1 Components and measurement points in the ventilation system of the Mediå School.

## 2.1 Pressure differentials

Measuring very low pressure-differentials is not straightforward. Instruments available at the laboratory of Energy and Process Engineering, NTNU, were tested prior to the experiments. In order to avoid the risk of error and possible loss of accuracy associated with calibration of pressure transducers it was decided to apply pressure manometers directly. It was found that a combination between two types of manometers gave very good accuracy without any need for calibration. One was a classic sloping-manometer filled with alcohol and the other a heavy, stable manometer, here referred to as water manometer, with a very accurate reading-scale ( $\pm 0.1$  Pa). Both manometers are normally used in a laboratory environment in order to calibrate pressure transducers.

In the laboratory, the tubes connected to the manometers typically have an inner diameter of 1 mm. However, due to the tube-length needed in the field, problems with viscous friction and viscous damping in the tubes resulted in an unacceptable long response time when using this tube dimension. Initial testing and evaluation showed that increasing the inner tube diameter from 1 to 4 mm ensured an acceptable response time. This, as well as the installation of tubes and the other preparations made, is further described in [2].

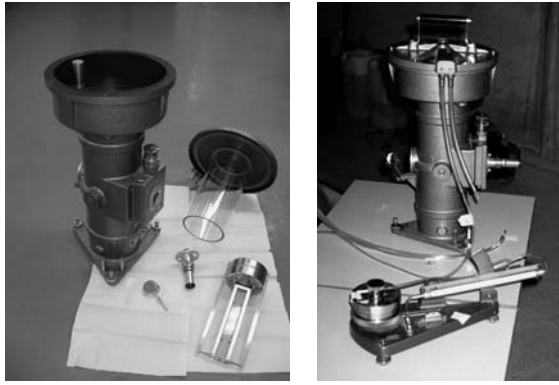


Figure 2 The water manometers were properly cleaned with distilled water prior to the field experiments (left). The manometers were used in combination with classic sloping manometers (right). One couple of manometers was placed in the extract chamber, and a second in the embedded distribution duct.

## 2.2 Airflow rates

It soon became clear that accurate measurement of the volumetric flow rate would be a more difficult task than that of measuring pressure differentials. Based on the assumption that the continuous fins would act as flow-directors at the entrance of the heating coil (point 5 in Figure 1), the following method was attempted:

Three of the four heating coils installed in parallel were tightened with plastic. The entrance of the remaining coil, which had an opening area of approximately  $1 \text{ m}^2$  was divided into 100 quadrants with exactly the same size.

The air velocity was then measured in the centre of each quadrant with a TSI Velocity Calc Plus velocity metre with accuracy of  $\pm 3\%$ . The measured velocity was then corrected for the actual temperature, and the airflow rate calculated as  $\sum V \cdot dA$ , where  $dA$  is the area of each quadrant.

The total time needed for the 100 measurements were 10 minutes. By repeating this method six times under nearly invariable conditions i.e. constant fan power and nearly constant temperatures, it was found that all the results differed by less than  $\pm 1.12\%$  from the mean value. This indicates a very high accuracy if one disregard possible systematic errors.

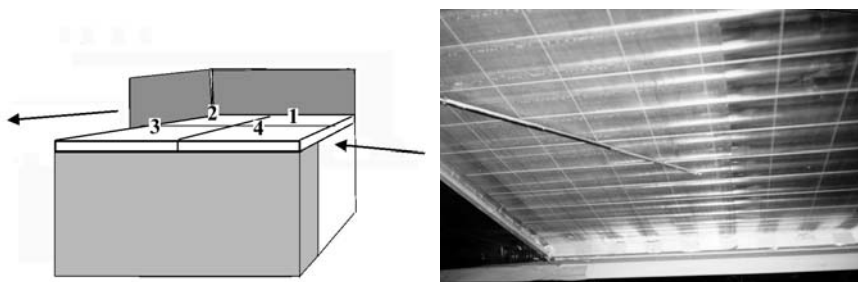


Figure 3 The combined heat recovery- and heating coil, with the main flow direction indicated (left). Coils number 2,3 and 4 were tightened with plastic for all except one measurement. 100 quadratic elements with identical surface area were sketched under coil number 1 (right). The velocity was then measured at the centre of each element.

However, in order to find the maximum airflow rate, one measurement was done with all the four parallel coils fully open and fans running at 100%. The same method was used

measuring 100 velocities for each coil and calculating  $\sum V \cdot dA$ . After having carried out the measurements for each of the four coils, the process was repeated for the coil number one. The difference was less than 1% between the airflow rate measured the first and the second time.

However, the airflow rate differed considerably for the different coils, with the lowest rate observed for element number 1 in Figure 3. For coil number 2,3 and 4, the air flow-rate was 1.33, 1.83, and 1.40 times higher respectively. The reason is probably that the coils are placed perpendicular to the flow direction. Due to the Bernoulli effect, element number 1 in Figure 3 will experience a pressure reduction at the entrance, limiting the airflow. At the same time, element number 3 will experience pressure reduction at the exit of the coil, increasing the airflow rate here.

### **3 Results and characterisation of the ventilation system components**

The general accuracy is considered to be within  $\pm 0.5$  Pa for the measured pressure differentials. Exceptions are measurements over the inlet vents in the inlet tower, as well as the combined outlet vents and heat recovery coil in the roof tower due to risk of wind influence. Based on the environmental conditions during the measurements, accuracy for these is considered to be within  $\pm 1.5$  Pa.

Disregarding possible systematic errors it is assumed that the airflow rate lies within  $\pm 5\%$  of the measurements. This is based on comparison between repeated measurements under invariable conditions as described in page 4 together with the accuracy of the instrument used ( $\pm 3\%$ ). When considering systematic errors the inaccuracy is higher however.

One measurement was done with the coil area fully opened and at maximum fan power. Measuring the air flow rate over all the four coil-units instead of one actually represents a change in method, and the possible systematic error mentioned above has to be taken into account. In addition, influence due to the direction of the flow will occur, see page 4, and this reduces accuracy even further. Thus  $\pm 20\%$  accuracy is assumed for this measured value.

All the curves have error bars, representing the inaccuracy, but note that the error bars for the pressure differentials in normal cases are so small that they are completely covered by the measurement points.

### 3.1 Pressure drop across the intake unit

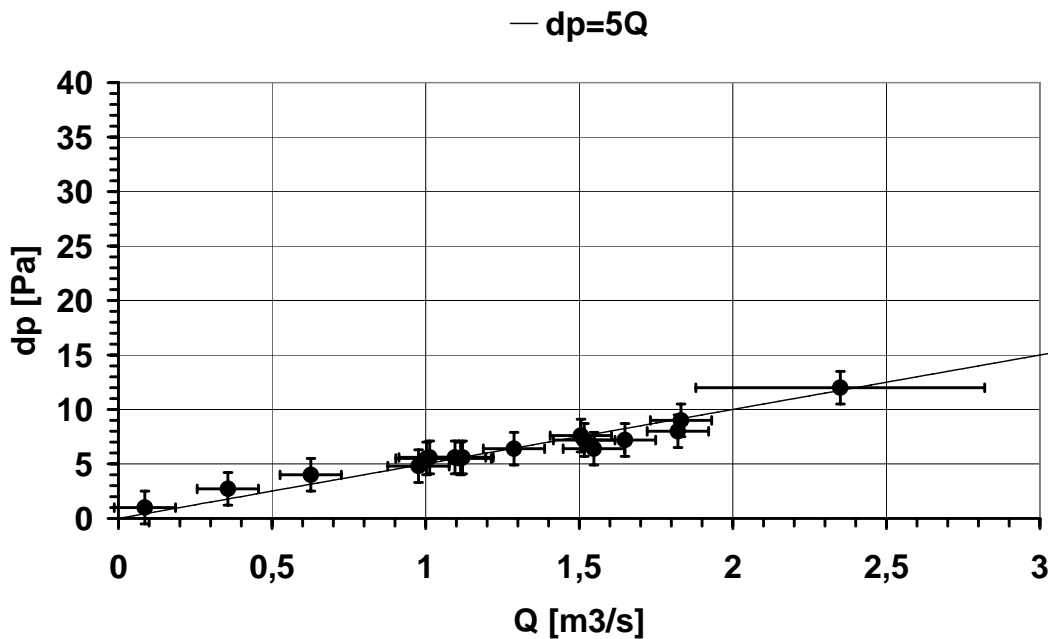


Figure 4 The pressure drop across the intake unit, consisting of the vents and openings in the intake tower.

Figure 4 shows the pressure drop over the inlet vents, and the openings in the inlet tower (point 1 in Figure 1). The inlet vents will dominate the flow resistance. They consist of square openings placed next to each other and equipped with a hatch that swings open due to the overpressure on its surface, preventing flow out of the tower in case of under-pressure. The weight of the hatches, as well as mechanical friction as they open, can therefore influence the resulting pressure differential over them.

At maximum airflow rate i.e. when  $Q$  is close to 2.5 m/s, the Reynolds number for each of these openings will be in the range 2000-4000, indicating that both viscous and turbulent effects can be expected.

As shown,  $\Delta p = 5Q$  seem to match the measurements well, and is proposed as an approximation for the characteristics. This indicates that viscous friction dominates over turbulent losses for this element.

### 3.2 Pressure drop across the filter

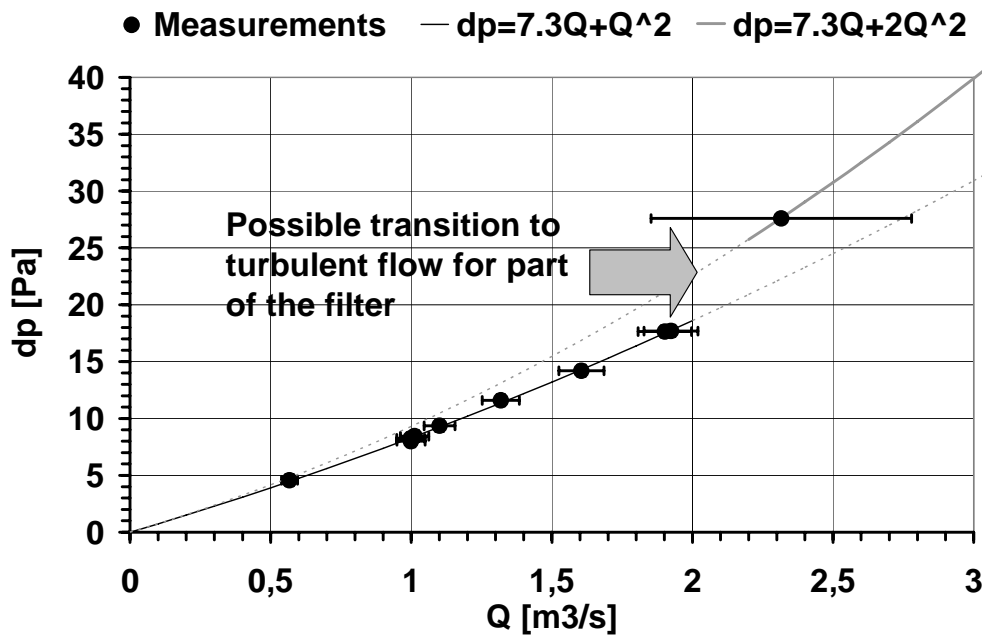


Figure 5 Pressure drop across the filter.

Figure 5 shows the pressure drop over the filter as a function of  $Q$ . Measurements matches the curve  $\Delta p=7.3Q+Q^2$  perfectly for  $Q$  lower than 2.0 m³/s. However, the measurement done at maximum airflow rate does not lie on this curve.

This can have two possible explanations. One is an error in the measurement of  $Q$ , as discussed above, so that  $Q$  should be close to 2.8 rather than 2.3 m³/s. The other is that there is a transition to turbulence for part of the flow through the filter somewhere between 2 and 2.3 m³/s, and a  $Q^2$  term should thus be added in order to match the measured point. This gives  $\Delta p=7.3Q+2Q^2$  for  $Q$  above 2.3m³/s.

The pressure differential for the other components at the maximum flow-rate of 2.32 m³/s seems to correspond well to their characteristics, supporting the hypothesis of turbulent transition.

Unfortunately, filter characteristics for pressure drops below 20 Pa have not been found when investigating data-sheets provided by various manufacturers. The existence of such a transition phase thus remains to be proven e.g. by experiments in a laboratory environment. Such experiments would also increase the general knowledge about the pressure drop over filters at very low airflow velocities and thus be beneficial for designers of low-pressure ventilation systems.

Under normal conditions during the heating season, the maximum airflow rate in the school never exceeds 1.5 m³/s since the fans are not allowed to operate at maximum speed due to noise problems. On hot days in summer, however, the heating coil and heat exchanger unit is bypassed in order to increase the airflow.

### 3.3 Pressure drop across the combined heat recovery and heating coil

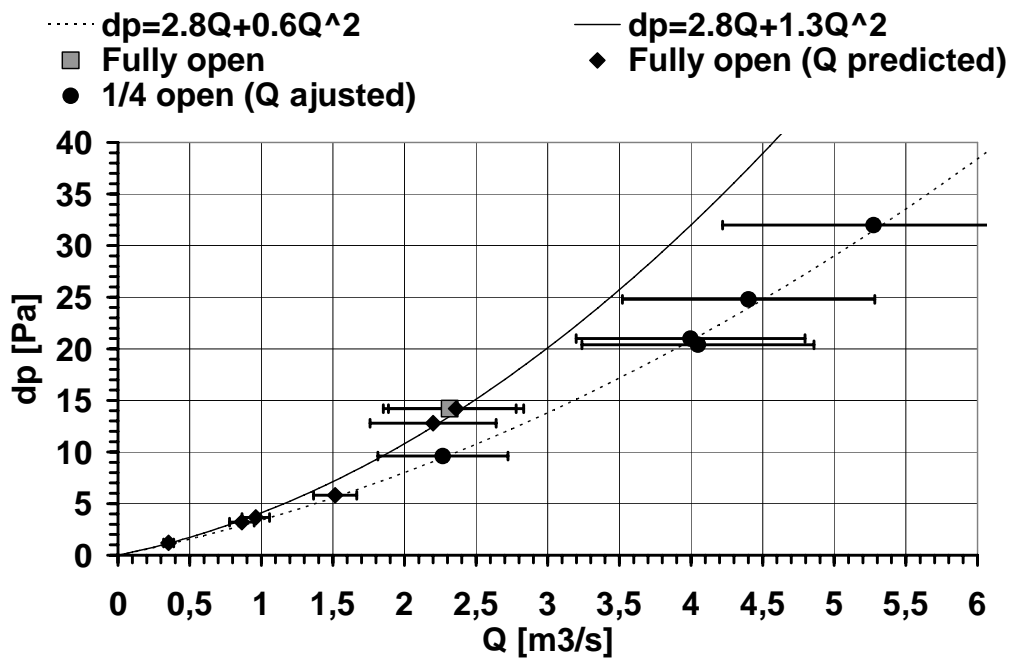


Figure 6 Measured pressure drop over the combined heat recovery- and heating coil at the Mediå School

Figure 6 shows the pressure drop over the combined heat recovery and heating coil. Almost all measurements were done with three of the four parallel coils tightened, see Figure 3. The characteristics of this coil element is therefore adjusted by replacing  $Q'$  with  $Q/4$  in  $\Delta p = f(Q')$ , where  $f(Q')$  is the characteristics for coil number one. As can be seen,  $\Delta p = 2.8Q + 0.6Q^2$  gives a nearly perfect match for these measured points.

However, the airflow through the four different coils varies considerably because the coils are placed perpendicular to the main airflow direction. An increased flow resistance is therefore expected.

The formula  $\Delta p = 2.8Q + 1.3Q^2$  matches the measurements done with all four coils fully open and fans running at maximum speed. The filter characteristic was used to estimate the lower airflow rates under these conditions. Except from one point (at  $Q = 1.52 \text{ m}^3/\text{s}$ ), the resulting points seem to fit  $\Delta p = 2.8Q + 1.3Q^2$  slightly better than  $\Delta p = 2.8Q + 0.6Q^2$ .

### 3.4 Pressure drop from the distribution duct to the extract chamber

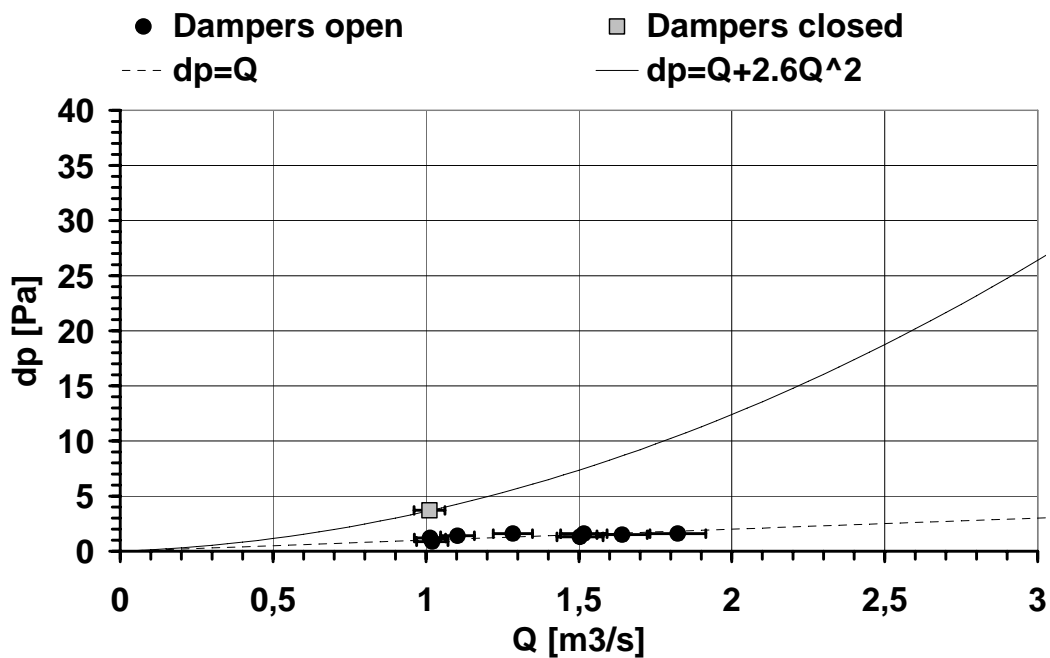


Figure 7 Pressure drop between the distribution duct and the extract chamber.

Figure 7 shows the pressure drop from the distribution duct to the extract chamber, i.e. from point 7 and 13 in Figure 1. Hatches were maintained fully open except for one measurement where they were in minimum opening position. Note that in order to provide background ventilation they are never allowed to close fully.

Considerations regarding these measurements, the corresponding airflow velocities and the design of the air supply openings indicate that viscous friction dominates caused by the air supply units dominates when the hatches are fully open. When the hatches “close”, minimizing the exhaust opening from the classrooms to the extract chamber, a turbulent contribution further reduces the airflow.

Thus, the supply resistance over the supply openings can be modelled as proportional to the airflow rate. The contribution from the exhaust openings can be neglected when the hatches are open, and modelled as standard airflow openings proportional to the square of the airflow rate when they are in closed position.

### 3.5 Pressure drop out through the roof tower

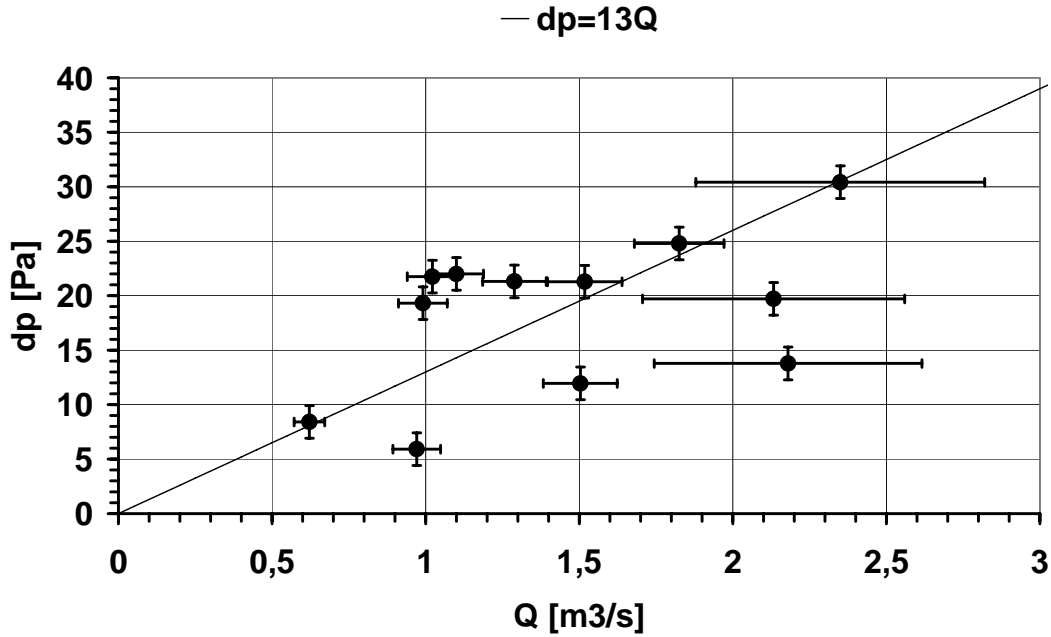


Figure 8 Measured pressure drop across the combined outlet vents and the heat recovery coil in the roof tower at the Mediã School.



Figure 9 Installation of measurement tube on the roof tower wall.

Figure 8 presents the measured pressure drop over the heat recovery coil and the outlet vents in the roof tower shown in Figure 9. The considerable spread in the measured values is due to wind influence. The geometry of the roof tower is triangular, with one heat-recovery coil on each side. The vents just outside the coils have a special design in order to prevent entrance of rain, snow and wind that would reduce the heat recovery effectiveness.

The design of these vents will not be shown here, but the measurements indicate that they are highly sensitive to wind even at low wind speeds. Recall that the measurements were done at low wind speeds, typically around 0.5 m/s. For unfavourable wind directions, vents on two sides can close. As a result, the total airflow is enforced out of only one of the heat-recovery coils, increasing the pressure drop by a factor of three or more.

Wind data at the time of the measurements were analysed. Unfortunately, no correlation that could be used to relate the wind speed and direction to the measured pressure drops was found. The formula  $\Delta p = 13Q$  is therefore proposed to represent the average pressure characteristics for the roof tower.

### 3.6 Fan characteristics

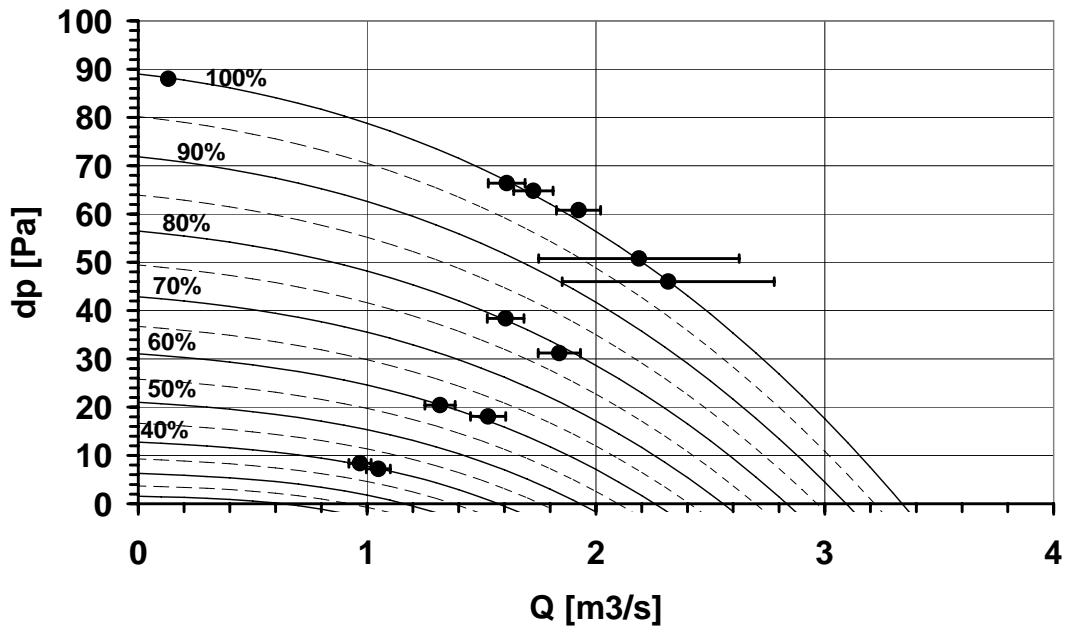


Figure 10 Measurements and fan characteristics for the supply fan at the Mediã School.

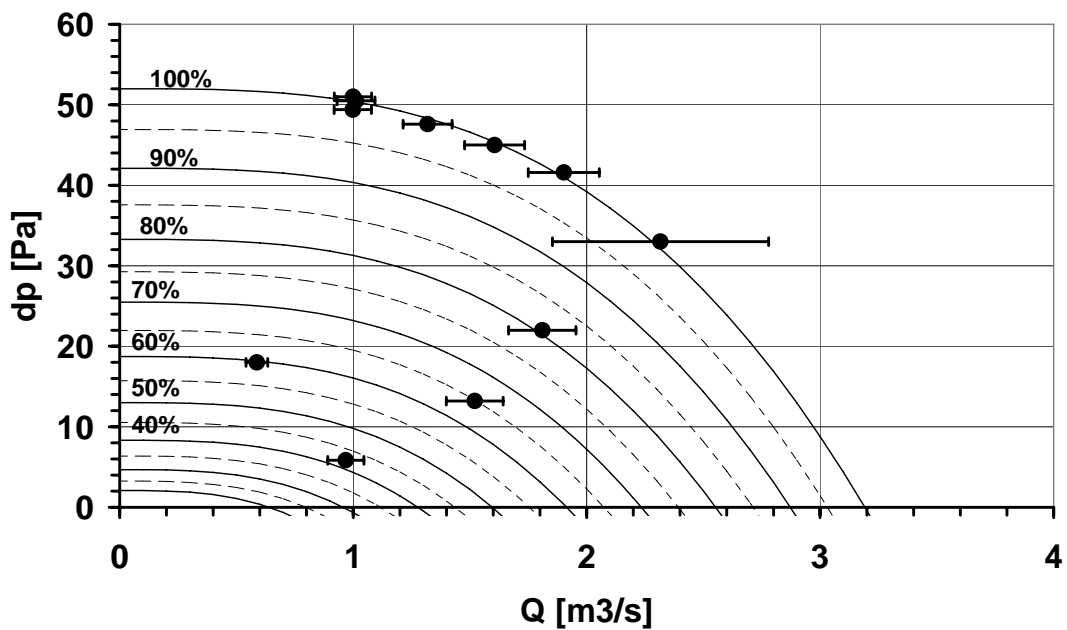


Figure 11 Measurements and fan characteristics for the extract fan.

Figure 10 and Figure 11 show the characteristics for the supply- and extract fan (points 2 and 14 in Figure 1) for different frequencies ( $n$ ) shown as a percentage of maximum frequency ( $n = np \cdot 100\%$  where  $np = \frac{n}{n_{MAX}}$ ). Note that due to noise problems, the supply fan is never allowed to operate are never allowed to operate at more than 85 % of its maximum frequency, while the limit for the extract fan is set to 70 %.

The characteristics are decided on the basis of measurements for the maximum frequency and adapted to the following polynomial expression:

$$\Delta p(Q) = \sum_{i=0}^3 a_i Q^i \quad (3-1)$$

In order to obtain characteristics for lower frequencies, an initial approximation is made by applying the affinity equations for axial compressors:

$$\frac{Q}{Q_{MAX}} = np$$

$$\frac{dp}{dp_{MAX}} = np^2 \quad (3-2)$$

$$\frac{P}{P_{MAX}} = np^3$$

$P$  is the delivered fan effect. This set of equations is valid if the fan efficiency is independent of  $np$ . For fan frequencies close to  $n_{MAX}$  i.e. when  $np$  is close to one, this is likely to be a good assumption. When the difference is important  $Q$  and hence the fluid velocities will be significantly reduced and the related head and friction losses can differ considerably from the situation with maximum fan frequency.

However, modifying the polynomial coefficients in Equation (3-1) according to the affinity equations gave very good results for the two axial fans at Mediå School, even for the lower frequencies. The polynomial fit coefficients  $a_0$ - $a_3$  were modified as follows:

$$a_i(np) = a_i)_{n=n_{MAX}} \cdot np^{2-i} \quad (3-3)$$

For the extract fan, the resulting fit coefficients are:

$$\begin{aligned} a_0(np) &= 52 \cdot np^2 \\ a_1(np) &= 0 \\ a_2(np) &= 0 \\ a_3(np) &= -1.6 \cdot np^{-1} \end{aligned} \quad (3-4)$$

Some minor modifications of Equation (3-3) are made in order to improve the accordance with the measurements for the supply fan:

$$\begin{aligned}
 a_0(np) &= 89 \cdot np^2 + 2.5 \cdot np - 2.5 \\
 a_1(np) &= -5.5 \cdot np^1 \\
 a_2(np) &= -4 - 5 \cdot np + 5 \\
 a_3(np) &= -0.7 \cdot np^{-1}
 \end{aligned}
 \tag{3-5}$$

Introducing Equations (3-4) and (3-5) into Equation (3-1) give complete polynomial expressions for the extract and supply fan for any fan frequency. In Figure 10 and Figure 11 they are plotted with 5% intervals from  $np=20\%$  to  $np=100\%$ .

### 3.7 System pressure characteristics

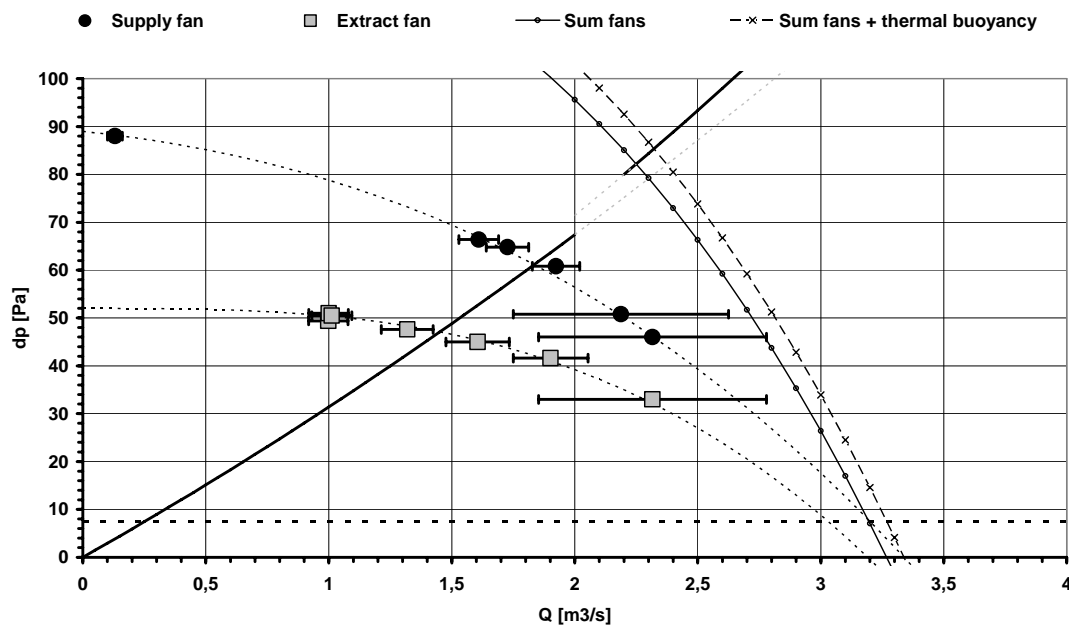


Figure 12 Total pressure drop for the ventilation system at the Mediå School (solid line) plotted together with the fan characteristics for the fans running at maximum speed, as well as the effect of thermal buoyancy (horizontal dashed line) for a particular moment. The sum of the pressure rise due to fans and thermal buoyancy (wind effects are neglected) must equal the system pressure drop. Thus, the system operates at the intersection between these two curves.

Formulae for the pressure drop over all components in the ventilation system at the Mediå School have now been empirically derived. Summing up, the pressure drop in the system can be expressed as:

$$\Delta P = 29.1Q + 2.3Q^2, \quad Q < 2
 \tag{3-6}$$

$$\Delta P = 29.1Q + 3.3Q^2, \quad Q > 2.3$$

when the hatches in the classrooms are in open position. From Figure 7 it can be seen that  $2.6Q^2$  should be added to these formulae when the hatches are closed. In addition, the fan openings will entail an additional resistance that should be taken into account when the fans are not operating.

In Figure 12, Equation (3-6) is plotted (solid line) together with the fan characteristics for both fans running at 100%. The volumetric flow rate measured when the supply and extract fan were operating at their maximum represent a capacity test of the system.

The effect of thermal buoyancy can be calculated accurately at any time since the temperatures in the ventilated rooms are monitored continuously. At the time of the capacity test, this effect was predicted to 7.5 Pa.

The measured airflow rate during the capacity test was  $2.32 \text{ m}^3/\text{s}$ . In Figure 12 it can be seen that the curve for the sum of the fans and thermal buoyancy intersects the curve for the system pressure drop exactly at this flow rate. This indicates that the measurements of the pressure differentials are correct

The horizontal dashed line in Figure 12 indicates the effect of thermal buoyancy at the time of the capacity test. It was predicted to 7.5 Pa. It can be seen that it intersects the system loss curve at  $0.25 \text{ m}^3/\text{s}$ , which is the flow-rate if the fans are turned off and the classroom hatches are left open.

## 4 Conclusions

The extremely low pressure drops and airflow velocities in buildings with natural ventilation make them difficult to measure accurately. Such measurements have been carried out for the hybrid ventilated Mediå School in Grong, Norway. The total ventilation airflow rate typically varies between 0.1 and 1.7 m<sup>3</sup>/s, in which range the total system pressure drop can be expressed as  $\Delta P = 29.1Q + 2.3Q^2$  [Pa], where  $Q$  [m<sup>3</sup>/s] is the airflow rate. This indicates that laminar flow dominates when the airflow rate is low i.e. when the fans operate at low speeds or in particular when the building is purely naturally ventilated. Turbulent friction, which normally dominates the pressure drop in conventional mechanical ventilation systems, can then be ignored.

Although the pressure drops in this particular hybrid ventilation system are very low compared to traditional mechanically ventilation systems, significant reduction in the total pressure drop could have been achieved through simple measures. For example increasing the cross sectional area of the filter, assembling the heat recovery coils placed within the roof tower vents to obtain more homogeneous flow through them and removing the inlet tower vents. If, at the same time, measures were made in order to utilise also wind as a driving force for the ventilation airflow, i.e. through optimisation of the inlet and roof tower design and placement, it is possible that sufficient airflow rates to assure the same indoor air quality as today in the classrooms could have been achieved without the use of fans. This can be investigated further through implementing the results into computer simulation tools with inter-zone airflow network models.

None the less, it can be concluded from this study that is fully possible to use regular mechanical ventilation components as filters and heat exchangers in a system based purely on natural driving forces. However, manufacturers of ventilation system components rarely carries out measurements at the low airflow velocities associated with natural ventilation. This is unfortunate for designers of natural ventilation systems. In particular, knowledge about the performance of filters at low airflow velocities is required. The results presented here indicate that there is a transition from turbulent flow to laminar flow through filters at low pressure drops.

## 5 References

- 
- 1 Tjelflaat, Per Olaf, *Pilot Study Report: Mediå School, Grong, Norway*, IEA ECBCS Annex 35:Hybvent.
  - 2 Wachenfeldt B. J (2003) *Natural Ventilation In Buildings, Detailed prediction of energy performance*, Department of Energy and Process Engineering, Faculty of Engineering, Science and Technology, NTNU, Dr. ingeniøravhandling (PhD thesis) 2003:72.